


Thermocline Dynamics in the Zone of the Rim Current Action in Winter Period (Based on to the Drifter Experiment Data)

A. A. Sizov , T. M. Bayankina, N. E. Lebedev

Marine Hydrophysical Institute, Russian Academy of Sciences, Sevastopol, Russian Federation
 *sizov_anatoliy@mail.ru*

Purpose. The paper is aimed at studying the thermocline response to slow (during a few days) and fast (up to two days) change of the current velocity, and also the process of changing in depth of the upper mixed layer lower boundary depending on the current velocity (at that the process is accompanied by the thickness and temperature gradient alteration in the thermocline).

Methods and Results. The thermocline responses were analyzed using the data on the upper layer temperature derived from the drifter experiment in 2012–2014. The drifters equipped with the thermal chains made it possible to measure temperature in the upper layer up to 80 m. The data covering the cold period (December – March) and obtained in five sub-regions in the Rim Current zone in the western and eastern parts of the sea were analyzed. The sub-regions were chosen proceeding from absence of the synoptic and mesoscale eddies in them. In each sub-region, the drifter position was estimated relative to the core of the Rim Current. Based on the mean daily sea temperature, the thermocline profiles were constructed, the thermocline boundaries, depth of the upper mixed layer lower boundary, the thermocline thickness and the temperature gradient in it were determined. The analysis showed that in case of a slow increase (decrease) in the current velocity, in all the sub-regions, there were a deepening (rise) of the upper mixed layer lower boundary, a decrease (increase) in the thermocline thickness and an increase (decrease) of the temperature gradient in it. This process is explained by possible propagation of the internal waves induced by the Rim Current velocity varying in the thermocline.

Conclusions. The results obtained showed that the fluctuation of the Rim Current velocity increased (decreased) the depth of the upper mixed layer lower boundary, the change of which was associated with an increase (decrease) in the thermocline thickness and in the temperature gradient in it. The drifters' data are significantly "noisy" due to the spatial inhomogeneities of the temperature field in the sea upper layer. Therefore, to obtain more accurate estimates of the processes, a study at the anchored measuring platforms installed in the zone of the Rim Current action is required.

Keywords: upper mixed layer, thermocline, geostrophic velocity, surface velocity, Rim Current, drifter

Acknowledgements: the investigation was carried out within the framework of the state task on theme No. 0555-2021-0002 "Fundamental studies of interaction processes in the ocean-atmosphere system conditioning regional spatial-temporal variability of natural environment and climate".

For citation: Sizov, A.A., Bayankina, T.M. and Lebedev, N.E., 2022. Thermocline Dynamics in the Zone of the Rim Current Action in Winter Period (Based on to the Drifter Experiment Data). *Physical Oceanography*, [e-journal] 29(1), pp. 67-82. doi:10.22449/1573-160X-2022-1-67-82

DOI: 10.22449/1573-160X-2022-1-67-82

© A. A. Sizov, T. M. Bayankina, N. E. Lebedev, 2022

© Physical Oceanography, 2022

Introduction

A detailed analysis of the processes of formation of the upper mixed sea layer (UML) during the autumn-winter mixing period is well described in [1, 2]. In recent years new technologies have significantly improved the understanding of the mechanism of turbulent mixing of the upper sea layer [3–5]. Use of drifting buoys with chain of thertmistors (drifters) has opened up new possibilities in the study of the UML and thermocline in the Black Sea Rim Current (RC) area [6].



The data of satellite altimetry and shear stress for calculating the geostrophic and drift components of the current velocity [7, 8] and the data of thermistors chain equipped drifters permitted to obtain estimates of the thermal state of the upper sea layer and the response of the thermocline to Rim Current velocity fluctuations [9]. In [10, 11] it was shown that with an increase in the Rim Current velocity, the UML thickness in the sea center decreases, while at the sea periphery in the Rim Current coverage area it increases. The results of studies [9–11] show that the thermocline depth varies depending on the Rim Current velocity. However, the very mechanism of the process leading to thermocline deformation in the Rim Current action zone remains opened to speculation.

In the present paper, following the earlier studies*, an attempt to find an explanation for the mechanism that causes a change in the depth of the upper boundary of the thermocline (UML lower boundary), as well as its thickness and temperature gradient in it, depending on the Rim Current velocity, is carried out.

Material used and processing technique

Geostrophic and surface velocities in the Rim Current area, simulated from satellite altimetry data [7, 8], were selected from oceanographic data array stored in the MHI Oceanographic Data Bank. From the same array, data on the temperature of the upper layer, obtained from thermistors chain equipped drifters, were selected.

To analyze the thermocline reaction to the current velocity change, those sections of the drifter trajectory were selected where they were not captured by synoptic or mesoscale eddies, but moved in the Rim Current core in December 2012 – February 2014. Five such sections (subregions) were selected: three in the western part, one in the eastern part of the Black Sea and one near the Southern Coast of Crimea (SCC) (Fig. 1). The December 2012 – February 2014 time interval was analyzed. The conditions corresponding to the hydrological winter (January – March), when due to density convection and turbulent mixing, the UML lower boundary (upper boundary of the thermocline) was maximally deepened [10, 11], were chosen.

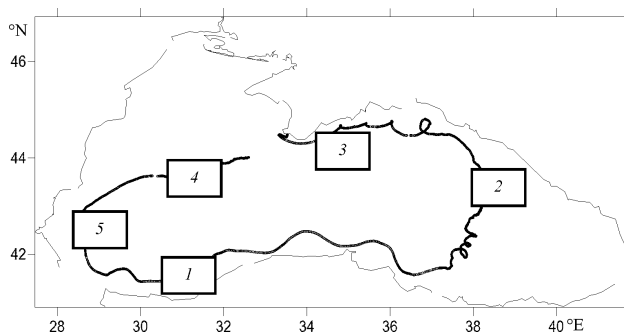


Fig. 1. Drifter trajectories. The numbers indicate the sub-regions for which the calculations were done

* Sizov, A.A., Bayankina, T.M. and Lebedev, N.E., 2020. Dynamics of the Depth of the Upper Boundary of the Seasonal Thermocline Depending on the Black Sea Rim Current Velocity (according to Satellite Altimetry and Drifter Experiment). *Sovremennye Problemy Distantionnogo Zondirovaniya Zemli iz Kosmosa*, 17(4), pp. 231-237. Available at: http://d33.infospace.ru/d33_conf/sb2020t4/231-237.pdf [Accessed: 15 January 2022] (in Russian).

Depth of the upper boundary of the thermocline (UML lower boundary) was estimated from the average daily sea temperature profiles. The accuracy of determining the thermocline boundaries was ensured by the distribution of temperature sensors on the thermal chain: its upper sensor was located at a depth of 0.2 m, the next – at depths of 10; 12.5; 15 m and further after 5 m to a depth of 80 m [6, 10]. Since the UML temperature changes smoothly, the thermocline boundaries were determined with an accuracy of ± 5 m. Thermocline thickness ΔZ (m) and the temperature difference in it ΔT ($^{\circ}\text{C}$) were estimated from these boundaries, followed by the temperature gradient $\Delta T/\Delta Z$ ($^{\circ}\text{C}/\text{m}$) calculation. For the convenience of analysis, the studied parameters were non-dimensionalized. The specific scales of the current velocity anomalies variability ($V_p = 0.1$ m/s), the depth of the UML lower boundary ($Z_p = 1$ m), the thermocline thickness ($\Delta Z_p = 1$ m), and the temperature gradient in the thermocline ($(\Delta T/\Delta Z)_p = 0.01$ $^{\circ}\text{C}/\text{m}$). The dimensionless values of the thermocline characteristics are marked with the symbol "*".

For each subregion (Fig. 1), the position of the drifter relative to maximum velocity (core) zone of the Rim Current was estimated. For this purpose, for the subregions, the calculation of the latitudinal variability of the geostrophic (surface) velocity on the meridians limiting the selected sections of the trajectory was carried out. For subsequent analysis, those sections of the drifter trajectory, on which it moved in the region of the maximum value of the Rim Current zonal velocity component, were selected. As an example, Fig. 2 shows the values of the zonal and meridional components of geostrophic velocity in subregion 1.

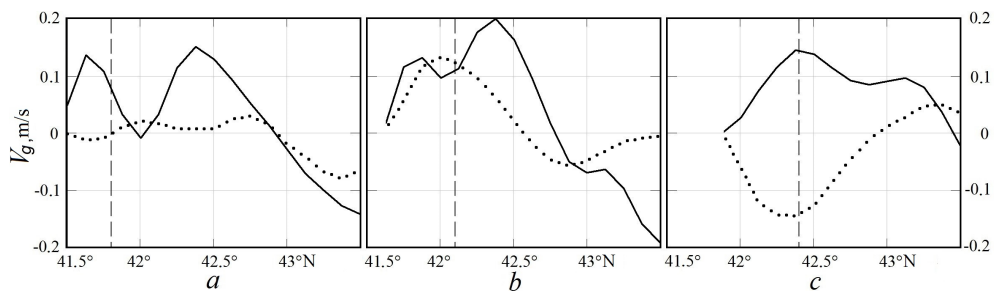


Fig. 2. Zonal (solid line) and meridional (dotted line) components of V_g , m/s in the sub-region 1 on 17.01.2013 (a), 19.01.2013 (b), and 22.01.2013 (c). Dashed lines show the drifter latitude position

Fig. 2 shows that during the entire analyzed time interval (January 17, 19, and 22, 2013), the maximum values of the zonal component of the geostrophic velocity were observed at the same latitudes the drifter trajectory passed at.

Results and their analysis

Before considering the variability of the UML depth (the upper boundary of the thermocline) depending on the changing current velocity, it had to be admitted that these processes in the selected subregions occurred in different time intervals of the hydrological winter. Subregions 1–3 are characterized by processes developing from the second half of January to the end of March, and in subregions 4 and 5, processes characteristic of the hydrological winter beginning (December –

first half of January) were observed. In addition, subregions 4 and 5 in the western part of the sea, are located in the area of the northeastern wind, largely determining the Rim Current intensity [10, 11]. At the same time, in subregions 1–3, the depth variability of the UML lower boundary was significantly associated with the geostrophic velocity fluctuation and insignificantly, with the surface velocity variability. At the same time, the depth of this boundary in subregions 4 and 5 significantly changed under the influence of the surface current velocity.

Fig. 3 shows graphs of average daily depths of the UML lower boundary and current velocity. It is important to note that in subregion 1 in the second half of January – early February 2013 and 2014 and in sub-region 5 in January 2013 and 2014, measurements were carried out by two drifters. This made it possible to compare hydrological processes in different years. Fig. 3, *a* shows the thermocline depth change depending on the geostrophic velocity in subregion 1. It is clearly seen that the negative trend of the geostrophic velocity from February 1, 2014 to February 10, 2014 was accompanied by the rise of the UML lower boundary to shallower depths. The same pattern of variability in geostrophic velocity and thermocline depth was observed in January 2013 (Fig. 3, *b*). Note that this process cannot occur due to UML convective mixing weakening, since density convection and turbulent mixing in the middle of winter can only increase the UML thickness [1, 2]. An estimate of the average daily variability of the UML lower boundary depth depending on the geostrophic velocity, obtained from data for February 6–8, 2014 (Fig. 3, *a*), shows that a decrease in velocity by 0.06 m/s was accompanied by an increase in the UML lower boundary by 8 m.

In subregion 2 (Fig. 3, *c*), the geostrophic velocity increase was accompanied by a deepening of the UML lower boundary. Here, the average daily increase in geostrophic velocity was determined from data for March 5–7, 2013. The results showed that an increase in geostrophic velocity by 0.09 m/s caused an increase in the depth of the UML lower boundary by 8 m.

Near the SCC (Fig. 3, *d*), the average daily increase and decrease in geostrophic velocity were determined from the data for March 26–28 and March 28–30, 2013, respectively. Estimates showed that with an increase in geostrophic velocity by 0.06 m/s, the UML lower boundary deepened by 5 m, and a decrease in velocity by 0.02 m/s was accompanied by a rise in this boundary by 5 m. Variability of the depth of the UML lower boundary depending on current velocity is also confirmed by measurements in subregions 4, 5 (Fig. 3, *e*, 3, *f*), where its drift (surface) component was used as the current velocity.

Fig. 3, *e*, *f* demonstrates that surface velocity increase led to a deepening of the UML lower boundary, while the velocity decrease led to its rise to smaller depths. Estimates of changes in the depth of the UML lower boundary depending on the geostrophic and surface velocities are very approximate. Taking into account the accuracy of determining the UML lower boundary depth (± 5 m), the above estimates show that drifter thermal chain sensors can detect changes in the UML lower boundary, starting from a change in the current velocity of about 0.1 m/s. Apparently, this can explain the existence in Fig. 3, *a*, *f* sections with constant depths of the UML lower boundary at a changing current velocity.

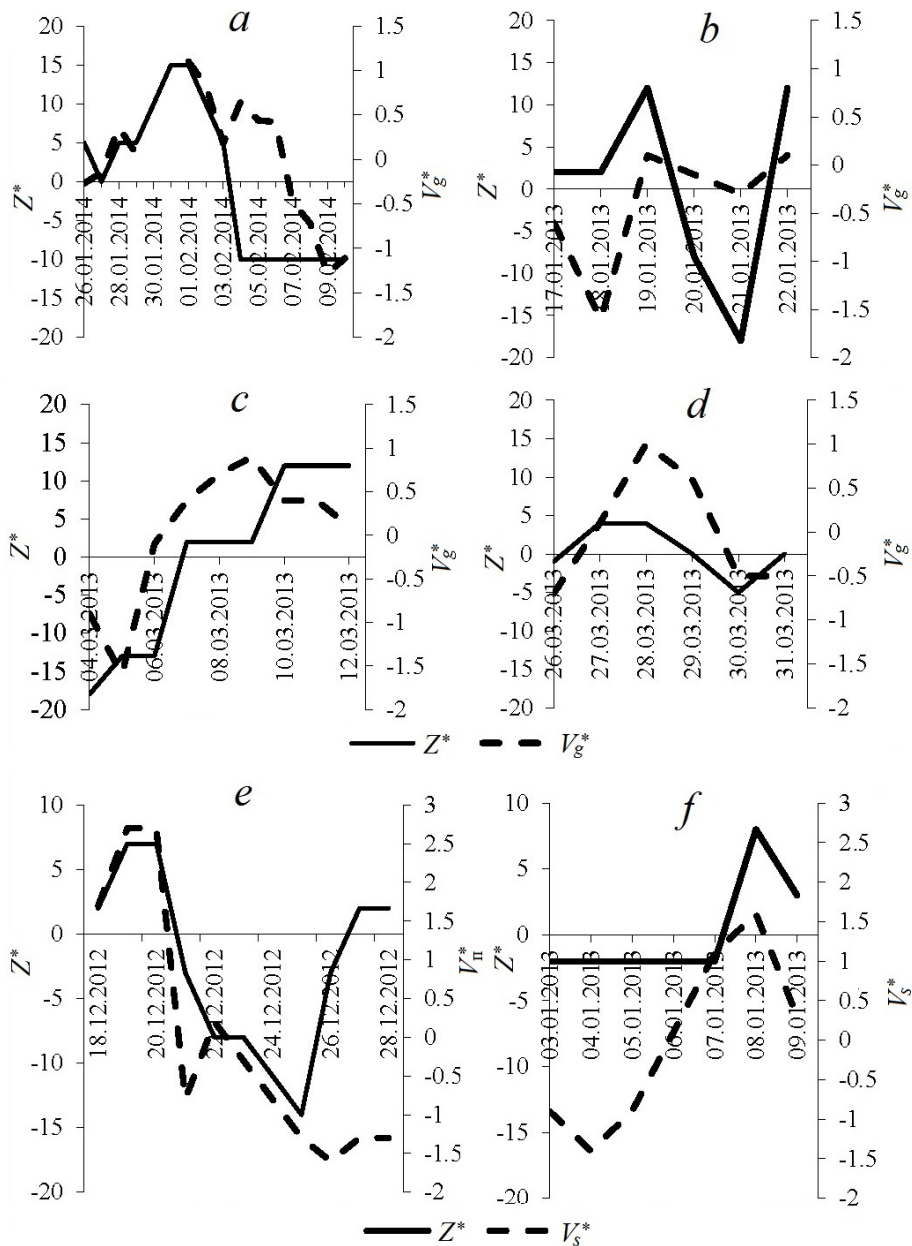


Fig. 3. Depth of the UML lower boundary (Z^*) depending on the current geostrophic velocity (V_g^*) in the sub-regions 1 (a, b), 2 (c), 3 (d) and the current surface velocity (V_s^*) in the sub-regions 4 (e) and 5(f)

It should also be borne in mind that the drifter, moving within the subregion boundaries, could fall into water masses with different physical characteristics, so the current velocity was not the only factor the position of the isotherms defining the lower boundary of the thermocline depended on. The Rim Current velocity change causes a change in the turbulent mixing intensity, which affects the position of the UML lower boundary and the thermocline characteristics. Nevertheless,

estimates show that the process of changing the depth of the UML lower boundary depending on the current velocity, recorded by the drifters' thermistor chain, is not accidental and is observed in the Rim Current zone both in the western and eastern parts of the sea.

On Fig. 3, *a* and 3, *e*, the attention is drawn to the processes of rapid (within one to two days) changes in the depth of the UML lower boundary depending on the current velocity. In subregion 1 (Fig. 3, *a*), geostrophic velocity decrease by 0.1 m/s from February 1 to February 3, 2014 was accompanied by the UML lower boundary rise by 10 m. In subregion 4 (Fig. 3, *e*), the surface velocity increase on December 18–20, 2012 by 0.05 m/s was accompanied by this boundary deepening by 5 m, and the current velocity decrease in on December 20–21 by 0.07 m/s was accompanied by the UML lower boundary rise by 5 m.

These processes of rapid (“impulsive”) change of the UML lower boundary depth are considered in [9]. There such a deformation of the thermocline was associated with an increase in the surface wind and, accordingly, the surface current when cold air masses enter the Black Sea. This intensified the total heat flux from the sea surface and turbulent mixing of the upper sea layer, which was reflected in the deepening of the UML lower boundary and its subsequent rise to smaller depths after the end of the cold intrusion.

The difference between the “impulse” deformation of the UML lower boundary and the slow one that occurs over several days will be shown by analyzing the variability of the thermocline thickness and the temperature gradient in it. It should be noted that the “impulse” process of the UML lower boundary deepening can also occur in the absence of a noticeable cooling of the sea surface due to the cold air intrusion of. In this case, the deformation of the lower boundary of the UML occurs due to a rapid increase in the flow velocity (Fig. 3, *f*).

The dependences of the UML lower boundary depth on the changing speed of the Rim Current, shown in Fig. 3, permit to present them in the form of a regression graph. For this, the geostrophic velocity deviations from its average value over the entire multi-day observation interval in each of subregions 1–3 were calculated. For subregions 4 and 5, surface velocity deviations were calculated. A number of dimensionless anomalies of the geostrophic velocity V_g^* and surface velocity V_p^* were obtained. A number of anomalies of the UML lower boundary depth Z^* were calculated in a similar way. According to the obtained dimensionless values – the anomalies V_g^* , Z^* and V_p^* , Z^* – regression plots were constructed (Fig. 4). Despite the significant scatter of the data, the correlation coefficient between the V_g^* and Z^* values was 0.64. In this case, the ratio of the correlation coefficient R to the error of its calculation (R/σ) was 6.4, which corresponds to the R significance at the level of 95% confidence. Linear approximation of the obtained dependence allows to express it as a regression relation $Z^* = 12.5 \cdot V_g^* - 2.5$. The correlation coefficient between the values of V_p^* and Z^* was 0.55, and the ratio $R/\sigma = 4.2$, which also corresponds to the R significance at the level of 95% confidence level. The linear approximation of the dimensionless depth of the UML lower boundary depending on the surface velocity can be represented as

$$Z^* = 4.8 \cdot V_p^* + 0.3.$$

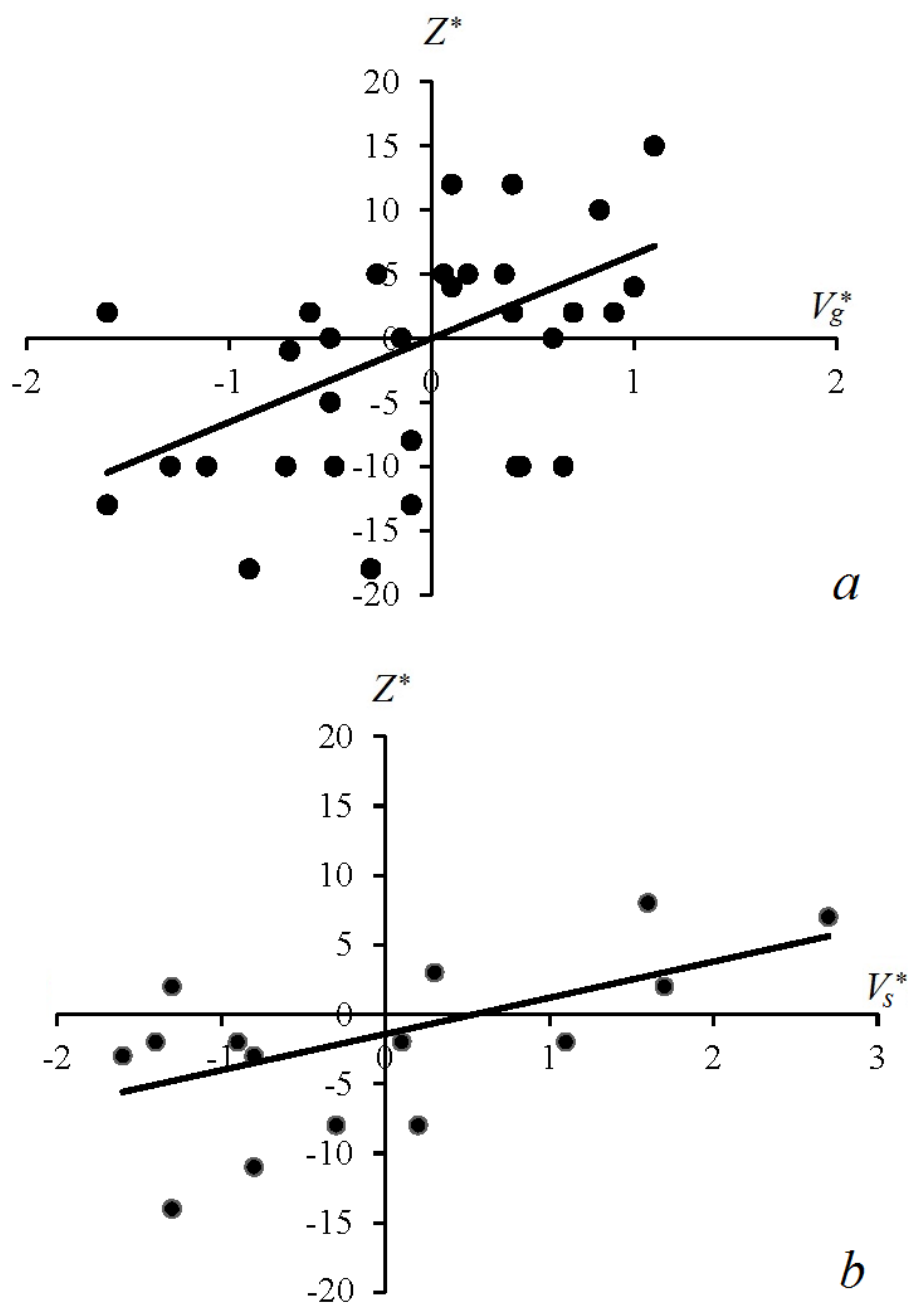


Fig. 4. Dependence of anomalies in the depth of the UML lower boundary on the current geostrophic velocity in the subregions 1–3 (a) and the current surface velocity in the subregions 4–5 (b)

Thus, the generalized anomalies Z^* , V_g^* and V_p^* given in Fig. 4 in subregions 1–5, located in the western and eastern parts of the sea, show that the geostrophic

and surface velocity increase in the Rim Current zone leads to a deepening of the UML lower boundary, and the velocity decrease causes it to rise to shallower depths. This result confirms the conclusions obtained in [9] for the western part of the sea. Along with the changing depth of the UML lower boundary in the Rim Current zone, the thickness of the thermocline and the temperature gradient in it also change. To estimate these parameters, data from all subregions were used, except subregion 3. Measurements in this subregion were carried out at the end of the hydrological winter, when the upper layer mixing reached its maximum depths, so the lower boundary of the thermocline was found to be at a depth exceeding the maximum length of the thermistors chain (80 m).

The change in the thermocline thickness depending on the depth of the UML lower boundary is shown in Fig. 5, where it is clearly seen that in subregion 2 (Fig. 5, *c*) the long-term deepening of the UML lower boundary on March 4–12, 2013 was accompanied by a trend towards the thermocline thickness decrease. This process looked more complicated in subregions 1 and 4, since in this case both long-term and short-term (“impulsive”) variability of the thermocline thickness was observed depending on the change in the depth of the UML lower boundary.

In subregion 1 (Fig. 5, *a*), a long-term rise in the lower UML boundary to shallower depths began on February 3, 2014 and was accompanied by the thermocline thickness increase until February 10, 2014. Until February 3, 2014, processes associated with an “impulsive” change in the depth of the UML lower boundary caused, as noted above, by the geostrophic velocity fluctuation, accompanied by UML intense mixing [9].

Apparently, this is the reason for the thermocline thickness increase observed during its deepening on January 29–31, 2014. After the short-term deepening of the UML lower boundary stopped and its rise to smaller depths on February 2–3, 2014, the thermocline thickness decreased. After February 3, a long-term rise of the UML lower boundary to shallower depths, accompanied by an increase in the thickness of the thermocline, began. The same pattern of “impulsive” deepening of the UML lower boundary, accompanied by the thermocline thickness increase, was observed in subregion 4 on December 18–19, 2012 (Fig. 5, *d*). It is clearly seen that the termination of the “impulsive” forcing on December 20–22 [9] led to the rise of the UML lower boundary to smaller depths, while the thermocline thickness decreased. On December 23–28, 2012, the process of long-term deepening of the UML lower boundary began. It was characterized by a tendency to the thermocline thickness decrease.

The data for subregion 5 show (Fig. 5, *e*) that the “impulsive” nature of the deepening of the UML lower boundary can apparently be realized even without noticeable convective mixing. This process can only be controlled by the changing surface current velocity. According to Fig. 5, *e*, the deepening of the UML lower boundary, observed on January 7–8, 2013, was accompanied by the thermocline thickness decrease and the rise of the UML lower boundary to shallower depths, occurred on January 8–9, was accompanied by the thermocline thickness increase.

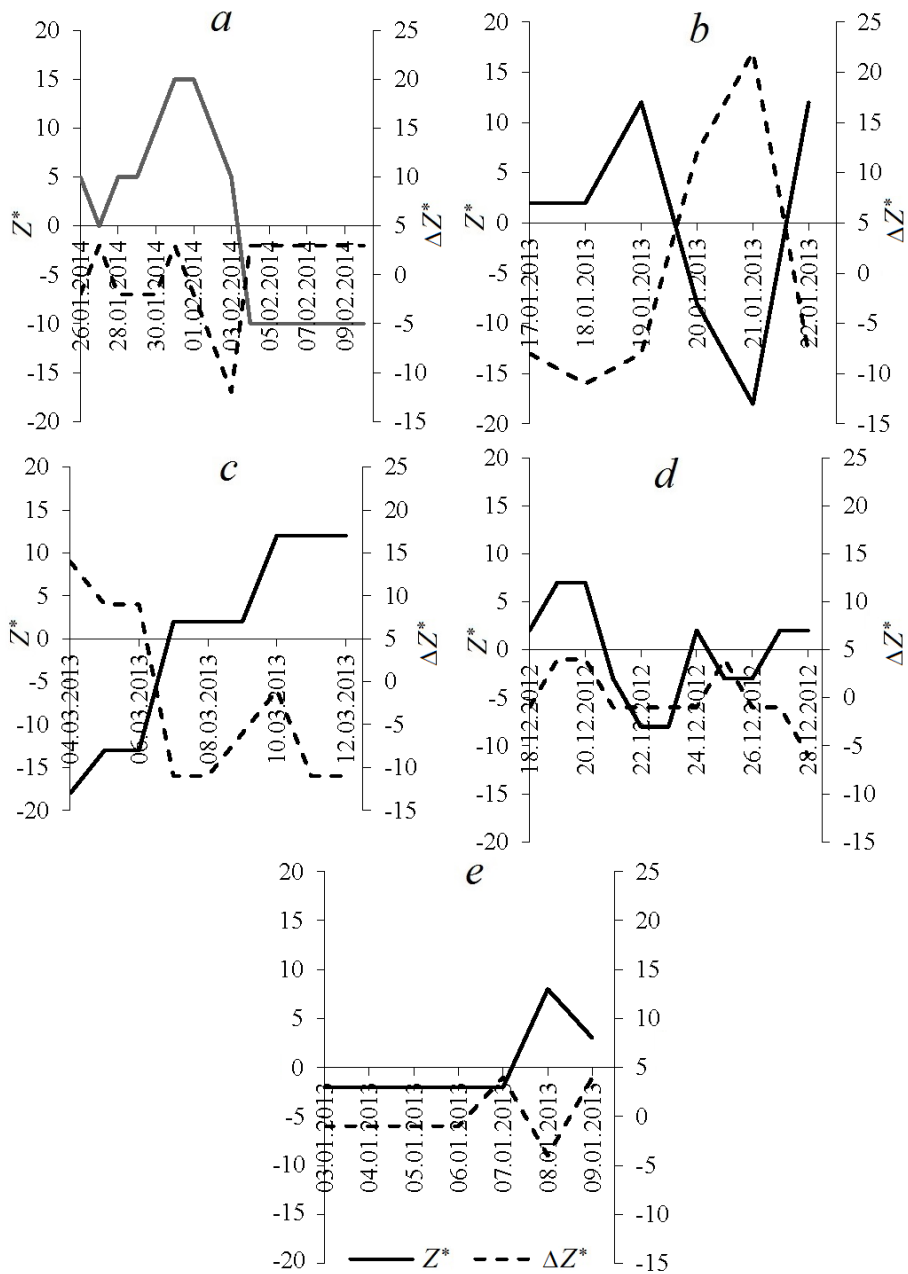


Fig. 5. Change in the thermocline thickness depending on the depth of the UML lower boundary in the sub-regions 1 (*a*), 2 (*c*), 4 (*d*) and 5 (*e*)

Change in the thermocline thickness depending on the change in the depth of the UML lower boundary, generalized for four subregions, is presented in the form of a regression graph in Fig. 6. To construct this graph, the dimensionless anomalies of the thermocline thickness ΔZ^* and the depth of the UML lower boundary Z^* , calculated in the same way as for constructing graph on Fig. 4, were used.

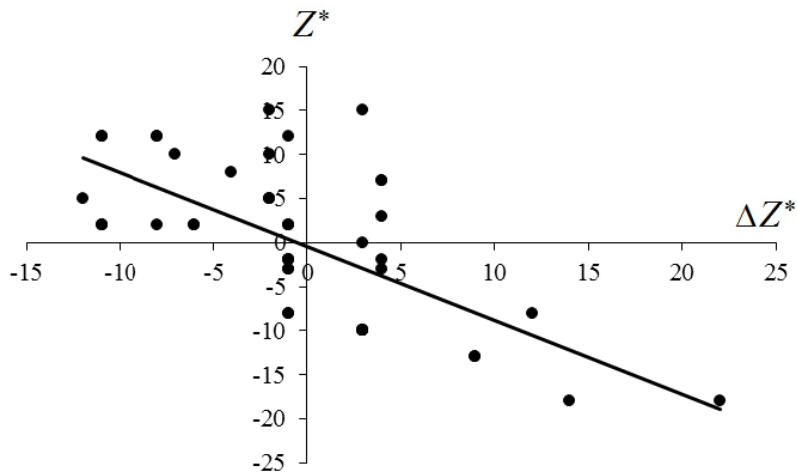


Fig. 6. Dependence of the thermocline thickness anomaly ΔZ^* upon the anomaly of the UML lower boundary depth Z^*

The graph in Fig. 6 was constructed from the array, which the data characterizing the short-term (“impulsive”) deepening of the UML lower boundary in subregions 1 and 4 were removed from. Thus, the regression graph (Fig. 6) represents the processes specific for the long-term subregions 1, 2, 4 and short-term variability Z^* in subregion 5. Therefore, Fig. 6 shows a steady trend towards a decrease in the thermocline thickness with the deepening of the UML lower boundary and its increase with the rise of the UML lower boundary to shallower depths. The linear approximation of this process is characterized by high values of the ratio of the correlation coefficient ($R = -0.76$) to the its calculation error ($R/\sigma = 11.7$), corresponding to the significance of the linear approximation at 99% confidence level. The regression graph $\Delta Z^*/Z^*$ can be represented as the ratio $\Delta Z^* = -0.69 Z^* - 1.33$.

Thus, the results in Fig. 6 allow to conclude that the process of long-term deepening of the UML lower boundary, observed with the current velocity increase in the Rim Current zone, is accompanied by a decrease in the thermocline thickness (thermocline compression). A long-term decrease in the depth of the UML lower boundary with the current velocity weakening in the Rim Current zone is accompanied by the thermocline thickness increase (thermocline expansion). This process is typical both for the multi-day regime of current velocity variability and for a short-term (“impulsive”) change in the current velocity, in which there is no intense mixing of the UML.

In the case of a short-term (“impulsive”) change in the current velocity, when intense UML mixing takes place during the cold air intrusion into the sea area, the process of thermocline deformation occurs in a different way [9]. In this case, when the UML lower boundary is deepened, the thermocline thickness increases (thermocline expansion), and when the UML lower boundary rises to shallower depths after the end of atmospheric forcing, the thermocline thickness decreases (thermocline compression).

A change in the thermocline thickness, caused by a change in the depth of the UML lower boundary and the current velocity in the Rim Current zone, leads to

a change in the temperature gradient in it. Thermocline compression with deepening of the UML lower boundary leads to the $\Delta T/\Delta Z$ value increase, thermocline expansion with a decrease in the depth of the UML lower boundary leads to $\Delta T/\Delta Z$ decrease. This process is presented in Fig. 7, which shows the situations in subregions 1 (Fig. 7, a, b), 2 (Fig. 7, c), 4 (Fig. 7, d) and 5 (Fig. 7, e). The dimensionless quantities Z^* and $(\Delta T/\Delta Z)^*$ were also used to construct the graphs.

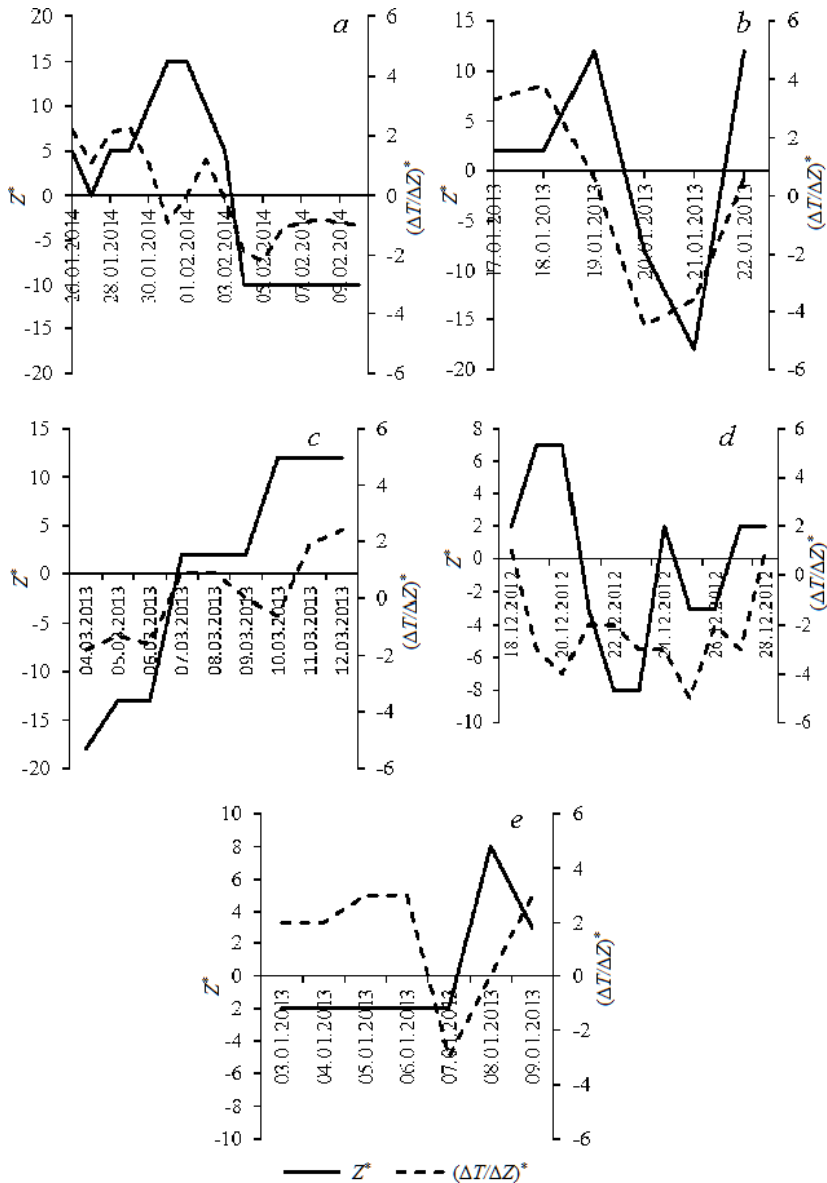


Fig. 7. Temperature gradient change $(\Delta T/\Delta Z)^*$ in the thermocline depending on the depth of the UML lower boundary Z^* in the sub-regions 1 (a, b), 2 (c), 4 (d) and 5 (e)

As can be clearly seen, the multi-day trend towards an increase in the depth of the UML lower boundary is specific for the current velocity increase and is accompanied by the temperature gradient rise in the thermocline. And vice versa, a multi-day trend towards a decrease in the depth of the UML lower boundary is accompanied by a tendency towards the temperature gradient decrease in the thermocline. With a short-term (within 1–2 days) change in the depth of the UML lower boundary, shown in Fig. 7, *b*, *d* (subregions 1, 4), the temperature gradient in the thermocline decreased with the deepening of the lower UML boundary on January 29–31, 2014 (Fig. 7, *b*) and on December 18–20, 2012 (Fig. 7, *d*). When the UML lower boundary was raised to shallower depths, the thermocline was compressed and, accordingly, the temperature gradient in it increased on February 1–3, 2014 (Fig. 7, *b*) and on December 22–29, 2012 (Fig. 7, *d*).

The presented relationship between the temperature gradient in the thermocline and the depth of the UML lower boundary is shown in Fig. 8 as a regression graph.

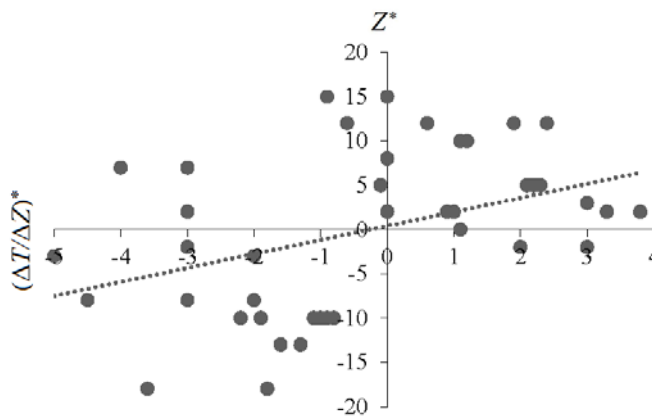


Fig. 8. Dependence of the temperature gradient $(\Delta T/\Delta Z)^*$ in the thermocline on the depth of the UML lower boundary Z^*

A noticeable data variability on the graph, partly due to the fact that both long-term and short-term changes in the depth of the UML lower boundary are presented here, nevertheless shows the characteristic variability of the analyzed parameters. In subregions 1, 2, 4, 5, the deepening of the UML lower boundary causes the thermocline compression and the temperature gradient increase in it, while the rise of the UML lower boundary to shallower depths is accompanied by the thermocline expansion and the temperature gradient decrease in it. The correlation between the temperature gradient $(\Delta T/\Delta Z)^*$ and the depth of the UML lower boundary Z^* is insignificant ($R = 0.41$), but the use of a relatively large amount of data ($N = 49$) makes it possible to reduce the error in calculating R . As a result, the value $R/\sigma = 3.4$, which makes it possible to consider the linear approximation of the dependence $Z^*/(\Delta T/\Delta Z)^*$ significant at 95% confidence level. This dependence can be represented as a ratio: $(\Delta T/\Delta Z)^* = 0.11 Z^* - 0.28$.

Discussion of the results and conclusion

The results obtained (Fig. 3–8) characterize the thermocline dynamics in the Rim Current action zone. Considering that the Rim Current intensifies in winter [4, 10–13], the obtained estimates of the UML lower boundary response to the Rim Current velocity change are valid for this time of the year. The drifter, whose sail is located at a depth of 10–15 m [6], moves in the area of the Rim Current maximum speeds [10]. Thus, the drifters' thermistor chains measure all the features of the vertical structure of the temperature field in the Rim Current area. Preliminary considerations on a possible mechanism for changing the depth of the upper thermocline boundary can be given taking into account the experiment described in [14]. The experiment showed that as the bottom current advances, characteristic undulating fluctuations are observed in the overlying layers of the stratified fluid. Later, the existence of such fluctuation introduced by near-bottom gravity currents into the overlying layers studied in [15]. In the present case, these results may be of interest if it is assumed that in a stratified fluid, being in the upper layer of the sea, the current propagates in the form of a submerged jet. In this case, it can be expected that the fluctuations arising in the boundary region of the jet will propagate both into the upper and lower layers of the sea. It is known that the vertical profile of the Rim Current shows the maximum values of the current velocity at a depth of 10–25 m, and the depth of the thermocline upper boundary varies in the range of 40–60 m [10]. The results obtained in the present paper and presented in Fig. 3 are consistent with these estimates. With this in mind, it can be assumed that the fluctuations introduced by the Rim Current jet into the area of maximum temperature gradients will be manifested more noticeably in the thermocline than in the UML, which was shown in Fig. 3.

Some confirmation of the reality of such a disturbance process can be found in [16], which analyzes the hydrological sections made by the R/V *Bilim* in the Rim Current area west of Crimea and near the Anatolian coast. We compared the velocities of the Rim Current and the positions of isotherms and isohalines in the current core area presented in this work. It turned out that at horizons shallower than the depth of the Rim Current axis, the isotherms and isohalines bent into the area of shallower depths. At the same time, the isotherms and isohalines in the thermocline, located deeper than the Rim Current axis, went down to greater depths. These results can be regarded as a qualitative confirmation of the assumption that it is possible to consider disturbances caused by the Rim Current as disturbances specific for the submerged jet boundary layer.

Below the results obtained in the selected subregions with climate estimates for the entire sea, made using the parameters taken from [10], are compared. For this purpose, such a similarity criterion as the Froude number is used: $Fr = V/(g'H)^{1/2}$, where V is the geostrophic or surface current velocity, m/s; g' is the reduced acceleration due to gravity; H is the depth of the UML lower boundary, m. The reduced acceleration of gravity is determined as follows: $g' = g\alpha\Delta T$, where $g = 9.8 \text{ m/s}^2$; α is the coefficient of thermal (volumetric) expansion, and ΔT is

the temperature difference at the upper and lower boundaries of the thermocline. The value of 0.15 m/s can be taken as a climatic estimate of the Rim Current velocity, the depth of the UML upper boundary is 35 m, and the temperature difference at the thermocline boundaries is 2.5 °C [10]. Taking the value of α equal to $1.5 \cdot 10^{-4} \text{ } ^\circ\text{C}^{-1}$, the Froude number values in the subregions are compared with its climatic value of 0.62:

Subregion	1	2	4	5
Fr	1.28	0.53	0.54	0.82

It is clearly seen here: in the western part of the sea in subregion 1, the Froude number exceeded the critical value, and in subregion 5 it approached it. This was mainly due to the relatively high average current velocity (more than 0.3 m/s). In the same subregions, there was a maximum depth of the UML lower boundary (46 and 50 m, respectively). In subregions 2 and 4, the Froude number was close to the climatic value, which is apparently typical for average current velocities of 0.2–0.25 m/s and the depth of the UML lower boundary of 35–40 m.

These selective estimates give reason to believe that there are other subregions in the Rim Current zone, non-included in our consideration, in which the Froude number will be less than the climatic value and in which the development of processes different from those described can be expected.

Conclusion

In conclusion, the preliminary results of the study of the thermocline response to the Rim Current velocity change are summarized. It should be noted that the information received from drifter thermal chains contains data on the spatial heterogeneity of the water masses which the drifter moves in. This introduces an additional noise effect, which reduces the accuracy of estimating the UML lower boundary response to the current velocity change. Nevertheless, the statistical reliability of estimates of thermocline depth changes depending on the current velocity suggests that this process requires targeted study. The mechanism that causes thermocline compression during its deepening and expansion during ascent to shallower depths in the case of a slow (over several days) change in the current velocity in the Rim Current area is not yet clear.

The materials of the drifter experiment and satellite altimetry used in this work do not allow to state that the Rim Current plays a significant role in the thermocline dynamics formation. More reliable estimates of these processes can be obtained by carrying out studies on stationary (moored) platforms placed in the Rim Current action area.

REFERENCES

1. Bulgakov, N.P., 1975. *Convection in the Ocean*. Moscow: Nauka, 272 p. (in Russian).
2. Dobrovolsky, A.D., Ed., 1977. *Convective Mixing in the Sea*. Moscow: University Press, 239 p. (in Russian).
3. Samodurov, A.S. and Chukharev, A.M., 2006. Estimation to Intensity of Vertical Turbulent Exchange in Upper Layer of the Black Sea according to In Situ Measurements. In: MHI, 2006. *Ekologicheskaya Bezopasnost' Pribrezhnykh i Shel'fovykh Zon i Kompleksnoe Ispol'zovanie Resursov Shel'fa* [Ecological Safety of Coastal and Shelf Zones and Comprehensive Use of Shelf Resources]. Sevastopol: ECOSI-Gidrofizika. Iss. 14, pp. 524-529 (in Russian).
4. Podymov, O.I., Zatsepin, A.G. and Ostrovsky, A.G., 2017. Vertical Turbulent Exchange in the Black Sea Pycnocline and Its Relation to Water Dynamics. *Oceanology*, 57(4), 492-504. <https://doi.org/10.1134/S0001437017040142>
5. Morozov, A.N. and Lemeshko, E.M., 2014. Estimation of Vertical Turbulent Diffusion Coefficient by CTD/LADCP-Measurements in the Northwestern Part of the Black Sea in May, 2004. *Morskoy Gidrofizicheskiy Zhurnal*, (1), pp. 58-67 (in Russian).
6. Tolstosheev, A.P., Lunev, E.G. and Motyzhev, S.V., 2014. Analysis of In-Situ Experiments with Temperature-Profiling Drifters in the Black Sea and Other Areas of the World Ocean. *Morskoy Gidrofizicheskiy Zhurnal*, (5), pp. 9-32 (in Russian).
7. Kubryakov, A.A. and Stanichny, S.V., 2011. Reconstruction of Mean Dynamic Topography of the Black Sea for Altimetry Measurements. *Issledovanie Zemli iz Kosmosa*,(5), pp. 24-30 (in Russian).
8. Kubryakov, A.A. and Stanichny, S.V., 2012. Reconstruction of Mean Dynamic Topography of the Black Sea for Altimetry Measurements. *Izvestiya, Atmospheric and Oceanic Physics*, 48(9), pp. 973-979. <https://doi.org/10.1134/S0001433812090095>
9. Sizov, A.A., Bayankina, T.M. and Yurovsky, A.V., 2019. Study of the Process of the Black Sea Upper Layer Mixing in the Zone of the Rim Current Activity in Winter Based on the Drifters Data. *Physical Oceanography*, 26(3), pp. 260-270. doi:10.22449/1573-160X-2019-3-260-270
10. Ivanov, V.A. and Belokopytov, V.N., 2013. *Oceanography of the Black Sea*. Sevastopol, 210 p.
11. Kubryakov, A.A., Belokopytov, V.N., Zatsepin, A.G., Stanichny, S.V. and Piotukh, V.B., 2019. The Black Sea Mixed Layer Depth Variability and Its Relation to the Basin Dynamics and Atmospheric Forcing. *Physical Oceanography*, 26(5), pp. 397-413. doi:10.22449/1573-160X-2019-5-397-413
12. Ginzburg, A.I., Zatsepin, A.G., Kostianoy, A.G. and Sheremet, N.A., 2008. Mesoscale Water Dynamics. In: A. G. Kostianoy and A. N. Kosarev, eds., 2008. *The Black Sea Environment*. Handbook of Environmental Chemistry, vol. 5. Berlin; Heidelberg: Springer, pp. 195-215. doi:10.1007/698_5_062
13. Kubryakov, A.A. and Stanichny, S.V., 2015. Seasonal and Interannual Variability of the Black Sea Eddies and Its Dependence on Characteristics of the Large-Scale Circulation. *Deep Sea Research Part I: Oceanographic Research Papers*, 97, pp. 80-97. doi:10.1016/j.dsr.2014.12.002
14. Maxworthy, T., Leilich, J., Simpson, J.E. and Meiburg, E.H., 2002. The Propagation of a Gravity Current into a Linearly Stratified Fluid. *Journal of Fluid Mechanics*, 453, pp. 371-394. doi:10.1017/S0022112001007054
15. Gritsenko, V.A. and Chubarenko, I.P., 2010. On Features of Structure of Bottom Gravity Current Frontal Zone. *Oceanology*, 50(1), pp. 28-35. <https://doi.org/10.1134/S0001437010010030>
16. Oguz, T. and Besiktepe, S., 1999. Observations on the Rim Current Structure, CIW Formation and Transport in the Western Black Sea. *Deep Sea Research Part I: Oceanographic Research Papers*, 46(10), pp. 1733-1753. [https://doi.org/10.1016/S0967-0637\(99\)00028-X](https://doi.org/10.1016/S0967-0637(99)00028-X)

About the authors:

Anatoly A. Sizov, Senior Research Associate, Marine Hydrophysical Institute of RAS (2 Kapitanskaya Str., Sevastopol, 299011, Russian Federation), Ph. D. (Phys.-Math.), **ORCID ID: 0000-0001-9055-4768**, sizov_anatoliy@mail.ru

Tatyana M. Bayankina, Research Associate, Marine Hydrophysical Institute of RAS (2 Kapitanskaya Str., Sevastopol, 299011, Russian Federation), Ph. D. (Geogr.), **ResearcherID: G-2535-2019**, bayankina@mhi-ras.ru

Nikolay E. Lebedev, Research Associate, Marine Hydrophysical Institute of RAS (2 Kapitanskaya Str., Sevastopol, 299011, Russian Federation), Ph. D. (Phys.-Math.)

Contribution of the co-authors:

Anatoly A. Sizov – formulation of the problem, analysis of variability of UML depth and thermocline characteristics depending on current velocity

Tatyana M. Bayankina – sampling of the Black Sea subregions and drifter thermococ data, calculation of the UML depth and thermocline characteristics according to drifter thermococ data

Nikolay E. Lebedev – calculation of geostrophic and surface velocities in the Black Sea subregions, estimation of drifter location relative to the zonal component of geostrophic velocity

All the authors have read and approved the final manuscript.

The authors declare that they have no conflict of interest.